Available online at www.sciencedirect.com
SCIENCE DIRECT®
PERGAMON
Polyhedron 22 (2003) 887–894
POLYHEDRON
www.elsevier.com/locate/poly

The X-ray structures of a series of copper(II) complexes with tetradentate Schiff base ligands derived from salicylaldehyde and polymethylenediamines of varying chain length

Lawrence C. Nathan *, Jessica E. Koehne, Joshua M. Gilmore, Kelly A. Hannibal, William E. Dewhirst, Tuyetha D. Mai

Department of Chemistry, Santa Clara University, 500 El Camino Real, Santa Clara, CA 95053, USA

Received 9 September 2002; accepted 28 December 2002

Abstract

The structures of six *N*,*N*′-polymethylene-bis(salicylaldiminato)copper(II) Schiff base complexes with alkyl backbones ranging from two to eight carbons have been determined by X-ray crystallography. The complexes are monomeric when the alkyl chain length is relatively short (two, three, and four CH_2 groups) but are dimers when the chain length becomes longer (five, six, and eight CH_2 groups). There is a regular increase in the distortion about the copper center as the alkyl chain length approaches four and five carbons, followed by a decrease as the chains become longer. Previously noted trends in electronic spectral, magnetic susceptibility, and microwave dielectric loss data can be accounted for based on this structural information.

Keywords: Copper; Tetradentate; Quadridentate; Schiff-base; Polymethylenediamine; Salicylidene

1. Introduction

Tetradentate Schiff bases derived from 2 equiv. of salicylaldehyde and 1 equiv. of a variety of alkyl or aryl diamines have been known for decades. Here we focus on those derived from polymethylenediamines with a regular progression of chain lengths as shown in the structural diagram below. In this paper, these compounds are abbreviated as H_2Sal-*n*, where *n* is the number of CH_2 groups in the amine backbone.

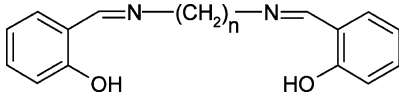

Through the loss of the two hydroxyl protons, these ligands have been used to form neutral complexes with a number of divalent metal ions. The structures of the resulting complexes have been inferred from solubility information and from magnetic and electronic spectral data, but few have been elucidated using X-ray crystallography, presumably owing to the insolubility of many of the longer chain species. Since questions regarding trends in magnetic and spectral data remain unanswered in the absence of definitive structural information, we chose to investigate a key series of these complexes. To place this work in context, the available structural information for M(Sal-*n*) complexes with $M = VO^{2+}$, Ni^{2+}, Co^{2+}, Zn^{2+}, Be^{2+}, and Cu^{2+} is summarized below.

All of the vanadyl complexes VO(Sal-*n*) with $n = 2$–10 range from green to gray in color and have a $\nu_{V=O}$ of about 980 cm^{-1} except for $n = 3$ which is yellow–orange and has a $\nu_{V=O}$ of 861 cm^{-1} [1]. The former are thought to be five-coordinate square-pyramidal complexes, a fact confirmed for VO(Sal-2) via its crystal structure [2]. In contrast, VO(Sal-3) has been shown by X-ray crystallography to have an infinite chain structure and six-coordinate vanadium centers (via V=O→V=O interactions) [3] but is thought to break up into five-coordinate monomers in chloroform [1]. VO(Sal-6) is the only member of the series which exhibits antiferro-

* Corresponding author. Tel.: +1-408-554-4949; fax: +1-408-554-7811.
E-mail address: lnathan@scu.edu (L.C. Nathan).

0277-5387/03/$ - see front matter
doi:10.1016/S0277-5387(03)00029-9

magnetic behavior at low temperature and VO(Sal-4) is the only one with two $\nu_{V=O}$ stretching modes, perhaps suggesting dimeric structures for both complexes. VO(Sal-2) is soluble in chloroform and pyridine, those with $n = 4$–6 are insoluble in chloroform and moderately soluble in pyridine, and those with $n = 7$–10 are minimally soluble in chloroform and readily soluble in pyridine, all of which suggest a variety of structures throughout the series. While it was concluded that compounds with $n = 4$–10 are not likely to be simple monomers, nothing more specific could be offered.

A limited number of nickel(II) complexes Ni(Sal-*n*) ($n = 2$–4) have been studied [4–6]. All are red–brown in color and diamagnetic, suggesting square-planar structures [4,5]. Electronic spectral data indicate that the ligand field strength decreases as the alkyl chain length increases [6]. Ni(Sal-2) does not react with pyridine while Ni(Sal-3) forms high spin Ni(Sal-3)$(py)_2$. Ni(Sal-3)$(H_2O)_2$ is also known and has a magnetic moment of $3.1\mu_B$. The latter two complexes are green and are proposed to be six-coordinate with *trans*-pyridine or water ligands [5].

Most of the members of the cobalt(II) series Co(Sal-*n*) ($n = 2$–10) precipitate immediately during synthesis and are insoluble in common solvents [7–10]. Co(Sal-2) has a magnetic moment of about $2.5\mu_B$ ($10^6\chi_m = 2750$) [7]; a partial crystal structure has shown it to be square-planar [8] which is consistent with the short two-carbon backbone. The other members of the series appear to be distorted- or pseudo-tetrahedral based on magnetic and solid-state electronic spectral data [9,10]. For example, compounds with $n = 3$–6 have magnetic moments in the 4.33–$4.56\mu_B$ range while those with $n = 7$–10 have magnetic moments in the 4.63–$4.68\mu_B$ range. All suggest tetrahedral-like structures, and although the complexes with the longer alkyl chains have slightly higher μ-values, there is no regular trend throughout the series. The conclusion drawn is that the longer alkyl chains allow adequate flexibility to form tetrahedral coordination geometries about the cobalt. Molecular ion peaks in the mass spectra indicate that the complexes with $n = 3$–6 are monomers, but the extreme lack of solubility might suggest otherwise. Also known is Co(Sal-3)$(H_2O)_2$; based on a magnetic moment of $5.52\mu_B$ it is proposed to have a monomeric *trans*-octahedral structure [10].

Zinc(II) also prefers tetrahedral coordination geometries in the H_2Sal-*n* series [11]. H_2Sal-2 has too short of an alkyl chain to achieve a true tetrahedral geometry, forcing the zinc to become five-coordinate. A crystal structure of Zn(Sal-2)(H_2O) shows zinc to have an approximately square-pyradmidal coordination environment with the water molecule in the axial position [12]. Anhydrous Zn(Sal-2) and Zn(Sal-3) have two IR bands in the 1560–1500 cm^{-1} region, interpreted as being indicative of both bridging and non-bridging C–O groups. A polymeric structure for these compounds was proposed with zinc being five-coordinate [11]. Electronic spectral data (ligand $\pi \rightarrow \pi^*$ transitions) indicate that these two complexes break apart and add pyridine to become five-coordinate monomers in solution. IR data for the zinc complexes with $n = 4$–6 and 9 suggest that they are tetrahedral, again owing to a more lengthy and flexible alkyl chain.

Beryllium(II) is equally intolerant of non-tetrahedral coordination geometries with H_2Sal-*n* ligands [13]. Be(Sal-2) and Be(Sal-3) could not be prepared, the products instead being Be$(HSal\text{-}2)_2$ and Be$(HSal\text{-}3)_2$. These complexes are thought to have two bidentate ligands coordinating through one oxygen and one nitrogen. It was concluded from IR spectra and molecular weight measurements that Be(Sal-4) and Be(Sal-6) are tetrahedral monomers.

The copper(II) series Cu(Sal-*n*) ($n = 2, 3, 4, 5, 6, 8, 10$) has been studied extensively [4,6,14–17]. Cu(Sal-2) has been shown by X-ray crystallography to be a 'stacked-dimer' with an elongated square-pyramidal coordination environment about copper [14]. The primary ligand coordinates in a *cis*-N_2O_2 mode, and there are two additional, longer Cu–O links connecting the two molecules. Available spectral and magnetic data are consistent with a square-planar coordination environment so perhaps the dimer breaks apart in solution and/or the longer Cu–O bonds have minimal impact on these properties. Electronic spectral data for the Cu(Sal-*n*) series in toluene reveal that the major d–d transition undergoes a red-shift from $n = 2$ to 4 (n, λ_{max} in nm: 2, 565; 3, 605; 4, 640), then reverses itself from $n = 4$ to 8 (n, λ_{max} in nm: 6, 615; 8, 600) [15]. Magnetic data parallel this trend with the maximum values in mid-series (n, μ_{eff} in μ_B: 2, 1.84; 3, 1.89; 4, 1.94; 6, 1.74) [4]. Panova, et al. [15] concluded that all complexes in the Cu(Sal-*n*) series were monomers with stereochemistries varying systematically from *cis*-planar ($n = 2$ viewed as a monomer), to distorted tetrahedral ($n = 3$), to tetrahedral ($n = 4$), to distorted tetrahedral ($n = 6$), to *trans*-planar ($n = 8$). In other words, the increasing chain length provides enough flexibility for the complexes to gradually 'invert' from a *cis*-planar configuration to a *trans*-planar configuration. Batley and Graddon [16] offered a slightly different conclusion—that there is a progressive distortion from planarity from $n = 2$ to 4 and that the longer chain members are polymeric. Similarly, Gruber, et al. [4] proposed that Cu(Sal-6) is polymeric. A recent study of microwave dielectric loss as a function of alkyl chain length parallels the magnetic and spectral data, showing first an increase then a decrease throughout the series (n, α'' in l mol^{-1}: 2, 0.04; 3, 0.125; 4, 0.27; 5, 0.27; 6, 0.20; 8, 0.17) [17]. The authors were unable to offer an adequate rationale for this trend in the absence of specific structural information.

Due to the scarcity of definitive structural information on H_2Sal-*n* complexes, we chose to study the structures of the Cu(Sal-*n*) series with $n = 3, 4, 5, 6, 8$ using X-ray crystallography. We have also redetermined the structure of Cu(Sal-2) to obtain more precise measurements than those reported in 1960 [14].

2. Experimental

2.1. Syntheses of ligands

All ligands were prepared by a standard method in which 2 equiv. (e.g. 20 mmol) of salicylaldehyde and 1 equiv. (e.g. 10 mmol) of the appropriate alkyl diamine are refluxed for 1–1.5 h in ethanol (about 50 ml). Upon cooling and/or reduction of the volume, yellow products are obtained in yields in excess of 70%. Products were verified by comparing with literature melting points (m.p.) [15].

2.2. Synthesis of copper complexes

Two general methods were used to synthesize the complexes in this study.

Method A: a traditional reflux method [15]: copper(II) acetate (5.0 mmol) in 25 ml of methanol is mixed with the ligand (5.0 mmol) also in 25 ml of methanol. The solution is heated on a hotplate or refluxed for 15–30 min., then cooled in an ice bath. Products are obtained in yields in excess of 50%.

Method B: a room temperature (r.t.), high dilution, slow addition method [18]: a solution of copper(II) acetate (0.60 mmol in 100 ml of methanol) is added over a period of 3–4 h to a solution of ligand (0.60 mmol in 700 ml of methanol) using a cannula. The volume is reduced using a rotary evaporator. Products are obtained in yields of about 60%.

2.2.1. Cu(Sal-2)

Method A; dark green; 52% yield; dec. pt. 121–122 °C. Calc. for $C_{16}H_{14}N_2O_2Cu$ (Expr.): C, 58.26 (58.62); H, 4.28 (4.46); N, 8.50 (8.43). Crystals were grown from nitromethane.

2.2.2. Cu(Sal-3)

Method A; olive green; 50% yield; dec. pt. 283–285 °C. Calc. for $C_{17}H_{16}N_2O_2Cu$ (Expr.): C, 59.37 (59.23); H, 4.69 (4.81); N, 8.15 (8.06). Crystals were grown from 1,2-dichloroethane–pentane.

2.2.3. Cu(Sal-4)

Method A; khaki green; 66% yield; dec. pt. 189–193 °C. Calc. for $C_{18}H_{18}N_2O_2Cu$ (Expr.): C, 60.41 (60.51); H, 5.07, (5.31); N, 7.83 (7.86). Crystals were grown from methanol.

2.2.4. Cu(Sal-4)

Method B; khaki green; 87% yield; dec. pt. 188–191 °C. Product not analyzed; assumed to be the same as from Method A based on dec. pt. and IR spectrum.

2.2.5. Cu(Sal-5)

Method A; khaki green; 63% yield; dec. pt. 129–130 °C. Calc. for $C_{19}H_{20}N_2O_2Cu$ (Expr.): C, 61.35 (61.08); H, 5.42 (5.72); N, 7.53 (7.29).

2.2.6. Cu(Sal-5)

Method B; khaki green; 61% yield; dec. pt. 129–131 °C. Calc. for $C_{19}H_{20}N_2O_2Cu$ (Expr.): C, 61.35 (61.03); H, 5.42 (5.55); N, 7.53 (7.14). Crystals were grown from methanol.

2.2.7. [Cu(Sal-6)]$_3$(H_2Sal-6)

Method A; khaki green; 94% yield; dec. pt. 308–311 °C. Calc. for $C_{80}H_{90}N_8O_8Cu_3$ (Expr.): C, 64.89 (65.06); H, 6.13 (6.31); N, 7.57 (7.43). Crystals could not be grown for this product.

2.2.8. Cu(Sal-6)

Method B; pea green; 64% yield; dec. pt. 233–235 °C. Calc. for $C_{20}H_{22}N_2O_2Cu$ (Expr.): C, 62.24 (61.75); H, 5.75 (5.81); N, 7.26 (7.15). Crystals were grown from dichloromethane–hexane.

2.2.9. Cu(Sal-8)

Method A; khaki green; 67% yield; dec. pt. 172–174 °C. Calc. for $C_{22}H_{26}N_2O_2Cu$ (Expr.): C, 63.82 (63.76); H, 6.33 (6.50); N, 6.77 (6.85). Crystals were grown from 1,2-dichloroethane–pentane.

2.3. X-ray crystallography

X-ray data on all compounds were acquired at ambient temperature using a Siemens/Bruker AXS P4 four-circle diffractometer with graphite monochromated Mo Kα radiation ($\lambda = 0.71073$ Å). The structures were solved by direct methods and Fourier difference maps [19]. Data were corrected for absorption using the semi-empirical method XABS2 [20]. Refinements were performed by full-matrix least-squares on F^2 [19]. For Cu(Sal-*n*) $n = 2, 3, 4, 5, 6$, all non-hydrogen atoms were refined anisotropically. Hydrogen atoms were added in ideal positions (C–H, 0.97 Å for alkyl, 0.93 Å for aromatic; $U_H = 1.2U_{\text{attached C}}$) and were not refined. There was minor disorder in the alkyl backbones in Cu(Sal-3), Cu(Sal-5) and Cu(Sal-6) which was modeled accordingly. Although crystals of Cu(Sal-8) appeared to be of good quality, they diffracted weakly. That, coupled with what appears to be a high level of rotational disorder within the unit cell, proved to be problematic. After numerous data collections on a variety of crystals, and extensive attempts to add

Table 1
Crystal data and structure refinement for Cu(Sal-2), Cu(Sal-3) and Cu(Sal-4)

Compound	Cu(Sal-2)	Cu(Sal-3)	Cu(Sal-4)
Molecular formula	$C_{32}H_{28}Cu_2N_4O_4$	$C_{17}H_{16}CuN_2O_2$	$C_{18}H_{18}CuN_2O_2$
Formula weight	659.66	343.86	357.88
Crystal description	dark green plate	dark green pillar	green–brown plate
Crystal size (mm)	0.14 × 0.14 × 0.04	0.34 × 011 × 0.10	0.30 × 0.20 × 0.10
Temperature (K)	298	298	296
Crystal system	monoclinic	orthorhombic	orthorhombic
Space group	*C*2/*c*	*Pna*2$_1$	*Pbca*
Unit cell dimensions			
a (Å)	26.727(5)	12.052(2)	10.389(2)
b (Å)	6.990(2)	17.992(3)	14.765(2)
c (Å)	14.752(3)	6.8929(7)	20.480(5)
β (°)	97.52(1)		
V (Å^3)	2732.4(12)	1494.7(4)	3141.3(10)
Z	4	4	8
D_{calc} (g cm^{-3})	1.604	1.528	1.513
F(000)	1352	708	1480
μ (mm^{-1})	1.604	1.469	1.401
Max/min transmission	0.938, 0.789	0.851, 0.549	0.869, 0.627
θ Range for data collection (°)	2.79–25.00	2.03–24.99	1.99–24.99
Index ranges	$-31 \le h \le 31$, $0 \le k \le 8$, $0 \le l \le 17$	$0 \le h \le 14$, $0 \le k \le 21$, $0 \le l \le 8$	$0 \le h \le 12$, $0 \le k \le 17$, $0 \le l \le 24$
Reflections collected	3265	2122	4000
Independent reflections, R_{int}	2411, 0.0487	1437, 0.0375	2771, 0.0867
Data/restraints/parameters	2411/0/190	1677/7/203	2771/0/208
Absolute structure parameter	n/a	−0.06(5)	n/a
Goodness-of-fit on F^2	1.011	1.021	0.986
R_1, wR_2 $[I = 2\sigma(I)]$ [a,b]	0.0529, 0.1081	0.0493, 0.1173	0.0716, 0.1220
a, *b* values in weighting [b]	0.0303, 0.0000	0.0548, 0.0000	0.0538, 0.0000
Largest difference peak, hole (e Å^{-3})	0.393, −0.389	0.369, −0.378	0.449, −0.457

[a] $R_1 = \Sigma\ ||F_o| - |F_c||/\Sigma\ |F_o|$.
[b] $wR_2 = [\Sigma[w(F_o^2 - F_c^2)^2]/\Sigma[w(F_o^2)^2]]^{1/2}$ where $w = 1/[\sigma^2(F_o^2) + (aP)^2 + bP]$ and $P = (F_o^2 + 2F_c^2)/3$.

appropriate restraints and model the disorder, a complete structural solution was not achieved [21]. Crystallographic data are summarized in Tables 1–3, and thermal ellipsoid plots [19] for Cu(Sal-*n*) with $n = 2$, 3, 4, 5, 6 are shown in Figs. 1–5, respectively. Hydrogen atoms have been omitted from all plots for clarity. Additional details are available via Section 4.

3. Results and discussion

As outlined in Section 1, the structures of very few *N*,*N*′-polymethylene-bis(salicylaldiminato) complexes are known definitively. Particularly for the Cu(Sal-*n*) series, there are some interesting trends in electronic spectral, magnetic, and microwave dielectric loss data which are more understandable now that the actual structures are known.

3.1. Cu(Sal-2)

While Hall and Waters acknowledged that Cu(Sal-2) was a dimer, they reported the molecular formula, molecular weight, and the number of molecules per unit cell ($Z = 8$) in terms of the monomer [14]. This would place the molecules in general positions in the *C*2/*c* space group. The structure is more correctly described as a stacked dimer as illustrated by Fig. 1 (with $Z = 4$ in *C*2/*c*, Wyckoff special position 'd'), in which there is an inversion center (at 1/4, 1/4, 1/2) between the copper centers. As shown in Table 3, the primary Cu–O and Cu–N bonds are in the 1.905–1.953 Å range while the Cu–O(2a) and Cu(a)–O(2) bonds are 2.423 Å. The coordination environment created by the primary ligand can be evaluated via the dihedral angle between the Cu–N(1)–O(1) and Cu–N(2)–O(2) planes from each half of that ligand. Here that angle is 12.2(2)°, indicating that the coordination environment is only slightly distorted from planarity. As mentioned previously, spectral and magnetic data are consistent with a square-planar environment, suggesting that the Cu–O(2a) and Cu(a)–O(2) interactions are weak.

3.2. Cu(Sal-3) and Cu(Sal-4)

As shown in Figs. 2 and 3, our results demonstrate that Cu(Sal-3) and Cu(Sal-4) are four-coordinate and monomeric as predicted independently by Panova [15] and Batley [16]. Panova reasoned that a longer and more flexible alkyl chain would allow distortion of the

Table 2
Crystal data and structure refinement for Cu(Sal-5) and Cu(Sal-6)

Compound	Cu(Sal-5)	Cu(Sal-6)
Molecular formula	$C_{38}H_{40}Cu_2N_4O_4$	$C_{40}H_{44}Cu_2N_4O_4$
Formula weight	743.82	771.87
Crystal description	grn–brn parallelepiped	grn–brn irreg. prism
Crystal size (mm)	0.33 × 0.14 × 0.10	0.38 × 0.32 × 0.24
Temperature (K)	298	298
Crystal system	monoclinic	tetragonal
Space group	$C2/c$	$P4_1$
Unit cell dimensions		
a (Å)	19.998(4)	13.386(1)
b (Å)	10.414(2)	13.386(1)
c (Å)	18.956(5)	20.786(4)
α (°)	90	90
β (°)	113.80(3)	90
γ (°)	90	90
V (Å^3)	3612.0(16)	3724.7(8)
Z	4	4
D_{calc} (g cm^{-3})	1.368	1.376
$F(000)$	1544	1608
μ (mm^{-1})	1.222	1.187
Max/min transmission	0.885, 0.608	0.752, 0.593
θ Range for data collection (°)	2.23–25.00	1.81–25.00
Index ranges	$-23 \le h \le 23$, $0 \le k \le 11$, $-22 \le l \le 22$	$-15 \le h \le 0$, $-15 \le k \le 15$, $-24 \le l \le 24$
Reflections collected	7503	14 960
Independent reflections, R_{int}	3158, 0.1113	3380, 0.0923
Data/restraints/parameters	3157/6/222	6562/68/455
Secondary extinction	0.0002(2)	n/a
Absolute structure parameter	n/a	0.01(2)
Goodness-of-fit on F^2	0.945	1.014
R_1, wR_2 $[I = 2\sigma(I)]$ [a,b]	0.0572, 0.1109	0.0474, 0.1069
a, b values in weighting [b]	0.0580, 0.0000	0.0504, 0.0000
Largest difference peak, hole (e Å^{-3})	0.300, −0.224	0.335, −0.310

[a] $R_1 = \Sigma\ ||F_o| - |F_c||/\Sigma\ |F_o|$.
[b] $wR_2 = [\Sigma[w(F_o^2 - F_c^2)^2]/\Sigma[w(F_o^2)^2]]^{1/2}$ where $w = 1/[\sigma^2(F_o^2) + (aP)^2 + bP]$ and $P = (F_o^2 + 2F_c^2)/3$.

coordination environment, and postulated specifically that Cu(Sal-2) has a *cis*-planar environment (with respect to the primary ligand), that Cu(Sal-3) is a distorted tetrahedron, and that Cu(Sal-4) is tetrahedral [15]. These conclusions are reasonably correct—there is increasing distortion about the copper center as measured by the aforementioned dihedral angle. For Cu(Sal-3) and Cu(Sal-4) the dihedral angles are 25.4(2)° and 42.6(3)°, respectively. One can see, however, that Cu(Sal-4) is distorted only about half-way to tetrahedral given that the dihedral angle would be 90° for a true tetrahedron.

The increased twisting of the coordination sphere from Cu(Sal-2) to Cu(Sal-4) seems to be restricted to changes in specific bond angles around the copper center (see Table 3). While there are no systematic changes in the Cu–O or Cu–N bond lengths nor in the *cis*-O–Cu–N and *cis*-O–Cu–O bond angles in this part of the series, the *cis*-N–Cu–N angle increases by about 17° and the *trans*-O–Cu–N angle decreases by 17°–27° as the coordination plane distorts.

3.3. Cu(Sal-5), Cu(Sal-6) and Cu(Sal-8)

Panova did not study Cu(Sal-5) but proposed that Cu(Sal-6) and Cu(Sal-8) are monomers in which the ligand has twisted such as to provide a distorted tetrahedral structure for Cu(Sal-6) and a *trans*-planar structure for Cu(Sal-8) [15]. Batley [16] and Gruber [4] both postulated that Cu(Sal-6) and other long-chain members were polymeric. As shown in Figs. 4 and 5, our results demonstrate that these conclusions are not entirely correct. Cu(Sal-*n*) where $n = 5$, 6 (from Method B), 8 are specifically dimers rather than monomers or more complex polymers. These differ from the 'stacked' type of dimer illustrated by Cu(Sal-2)—in the $n = 5$, 6, 8 series one end of two primary ligands are bonded to each copper center. While the crystallographic solution for Cu(Sal-8) is incomplete due to weakly diffracting crystals and an apparent high level of rotational disorder in the unit cell, it is clear from both the unit cell/density data and connectivity [21] that the molecules exist as dimers very similar to that shown for [Cu(Sal-6)]$_2$ in Fig. 5. The [Cu(Sal-5)]$_2$ and [Cu(Sal-8)]$_2$ dimers sit on crystallographic inversion centers while the [Cu(Sal-6)]$_2$ does not. All three complexes in this part of the series have distorted coordination environments: for $n = 5$ (one unique Cu center), 6 (two independent Cu centers per molecule), and 8 (from the unique half of the major component of the best defined molecule) the aforementioned Cu–N–O dihedral angles are 40.5(2)°, 23.8(2)°/35.3(2)°, and approximately 32°, respectively. All three complexes exhibit essentially a *trans*-N_2O_2 donor set which is consistent with the conclusions drawn by Panova [15]. It is surprising that each end of the [Cu(Sal-6)]$_2$ dimer has significantly different dihedral angles about its copper center while the dihedral angles in [Cu(Sal-5)]$_2$ and [Cu(Sal-8)]$_2$ are forced to be the same due to their inversion symmetry.

Again, there is no specific trend in Cu–O or Cu–N bond lengths in the [Cu(Sal-5)]$_2$ and [Cu(Sal-6)]$_2$ series (see Table 3). The *cis*-O–Cu–N bond angles show minimal change, but the *trans*-O–Cu–O and *trans*-N–Cu–N angles increase from 11° to 14° as the coordination plane flattens.

Table 3
Selected bond lengths (Å) and bond angles (°) in the Cu(Sal-*n*) series

	Cu(Sal-2)	Cu(Sal-3)	Cu(Sal-4)	[Cu(Sal-5)]$_2$	[Cu(Sal-6)]$_2$	
					Cu(1)	Cu(2)
Bond lengths						
Cu–O(1)	1.905(3)	1.887(5)	1.895(6)	1.862(5)	1.883(4)	1.909(4) [a]
Cu–O(2)	1.946(3)	1.906(5)	1.902(6)	1.887(4)	1.890(4) [b]	1.891(4)
Cu–N(1)	1.953(4)	1.984(6)	1.987(7)	1.956(6)	1.967(4)	1.975(4) [c]
Cu–N(2)	1.952(4)	1.957(6)	1.938(7)	1.977(5)	1.979(5) [d]	1.959(5)
Cu–O(2a)	2.423(3)					
Bond angles						
O(1)–Cu–O(2)	91.4(2)	83.3(2)	87.5(2)	149.9(2)	153.0(2) [e]	160.8(2) [f]
N(1)–Cu–N(2)	83.8(2)	97.6(2)	100.8(3)	151.4(2)	155.9(2) [g]	165.4(2) [h]
O(1)–Cu–N(1)	92.4(2)	92.4(2)	94.2(3)	94.4(2)	93.8(2)	91.9(2) [i]
O(2)–Cu–N(2)	91.1(2)	92.5(2)	93.1(3)	93.5(2)	94.0(2) [j]	92.5(2)
O(1)–Cu–N(2)	171.1(2)	160.1(3)	144.2(3)	93.2(2)	91.6(2) [k]	91.0(2) [l]
N(1)–Cu–O(2)	170.2(2)	160.7(4)	153.2(3)	93.5(2)	91.8(2) [m]	89.5(2) [n]

[a] Cu(2)–O(3).
[b] Cu(1)–O(4).
[c] Cu(2)–N(3).
[d] Cu(1)–N(4).
[e] O(1)–Cu(1)–O(4).
[f] O(2)–Cu(2)–O(3).
[g] N(1)–Cu(1)–N(4).
[h] N(2)–Cu(2)–N(3).
[i] O(3)–Cu(2)–N(3).
[j] O(4)–Cu(1)–N(4).
[k] O(1)–Cu(1)–N(4).
[l] O(3)–Cu(2)–N(2).
[m] N(1)–Cu(1)–O(4)
[n] N(3)–Cu(2)–O(2).

As indicated in Section 2, synthetic method A yielded a second form of Cu(Sal-6) which had a significantly higher decomposition point than the one from synthetic method B. The elemental analyses suggest a composition such as [Cu(Sal-6)]$_3$(H$_2$Sal-6), implying a rather complex structure. This synthesis was repeated four times with consistent results. Unfortunately, crystals could not be grown for this product. Cu(Sal-4) and Cu(Sal-5) were also prepared by both methods; in these cases the products were the same.

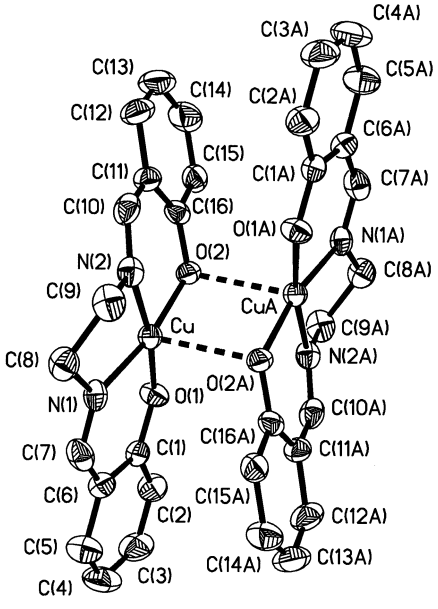

Fig. 1. Thermal ellipsoid plot at the 50% probability level for the stacked dimer [Cu(Sal-2)]$_2$. Hydrogen atoms are omitted for clarity.

3.4. Correlation with spectral and magnetic data

The structural results reported here make it possible to offer explanations for the observed trends in previously reported magnetic and spectral data for the Cu(Sal-*n*) series. First, the decrease then subsequent increase in ligand field strength from $n = 2$ to 8 (as reflected by λ_{max}) parallels the trend in distortion of the primary coordination environment about copper (as illustrated by the aforementioned Cu–N–O dihedral angles) from approximately planar to pseudo-tetrahedral and back toward planar. The correlation is quite good—Cu(Sal-2) has the highest energy d–d electronic transition ($\lambda_{max} = 565$ nm) and, with respect to the primary ligand, is most planar (dihedral angle = 12.2°), Cu(Sal-4) has the lowest energy d–d transtion ($\lambda_{max} =$

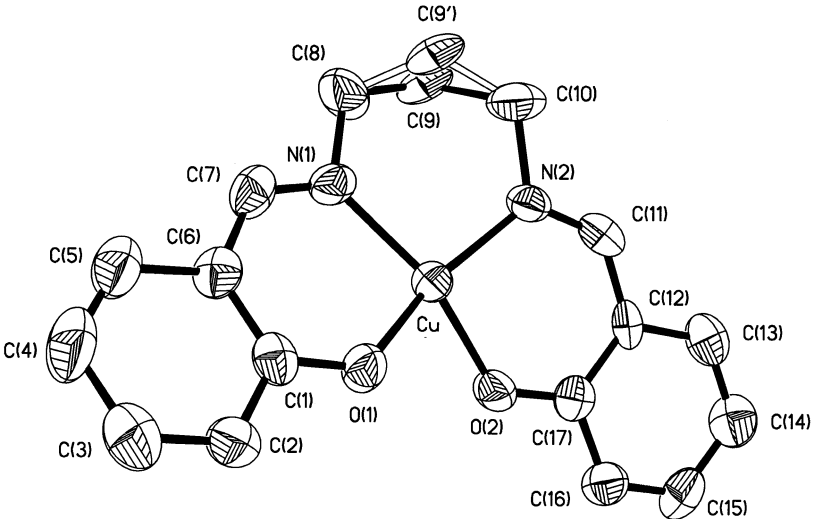

Fig. 2. Thermal ellipsoid plot at the 50% probability level for Cu(Sal-3). Hydrogen atoms are omitted for clarity. Disorder in the alkyl chain was modeled at 74% C(9) and 26% C(9′).

640 nm) and is least-planar (dihedral angle = 42.6°), while the d–d transition is intermediate for Cu(Sal-8) ($\lambda_{max} = 600$ nm) corresponding to intermediate planarity (dihedral angle $\approx 32°$). Second, since all of the Cu(Sal-*n*) complexes have one unpaired electron (with a spin-only moment of $1.73\mu_B$), the observed increase then subsequent decrease in magnetic susceptibility from $n =$ 2 to 6 is most likely due to the corresponding increase then decrease in the orbital contribution as the structures deviate more, then less, from planarity. Specifically, the least-planar complex Cu(Sal-4) has the largest magnetic moment ($1.94\mu_B$). In the dimeric structures, the copper centers are a minimum of 6.59 Å apart so no spin-coupling is anticipated. Finally, the maximum values of microwave dielectric loss (0.27 l mol^{-1}) occur with the most severely distorted complexes Cu(Sal-4) and Cu(Sal-5).

3.5. Conclusions

We have demonstrated that as the alkyl chain length increases in the series of Cu(Sal-*n*) complexes, the products can be characterized as follows: $n = 2$, a stacked dimer with the primary ligand in a *cis*-planar geometry; $n = 3$, monomeric, distorted *cis*-planar; $n = 4$, monomeric, distorted *cis*-planar or pseudo-tetrahedral; $n = 5$, dimeric, distorted *trans*-planar or pseudo-tetrahedral; $n = 6$, dimeric, distorted *trans*-planar; and $n = 8$, dimeric, distorted *trans*-planar. Based on these structural results, we have been able to correlate the observed trends in ligand field strength, magnetic susceptibility, and microwave dielectric loss to the degree of distortion from planarity about the copper center. In the Cu(Sal-*n*) series, we have shown that, with respect to the primary ligand, a monomer–dimer conversion occurs between

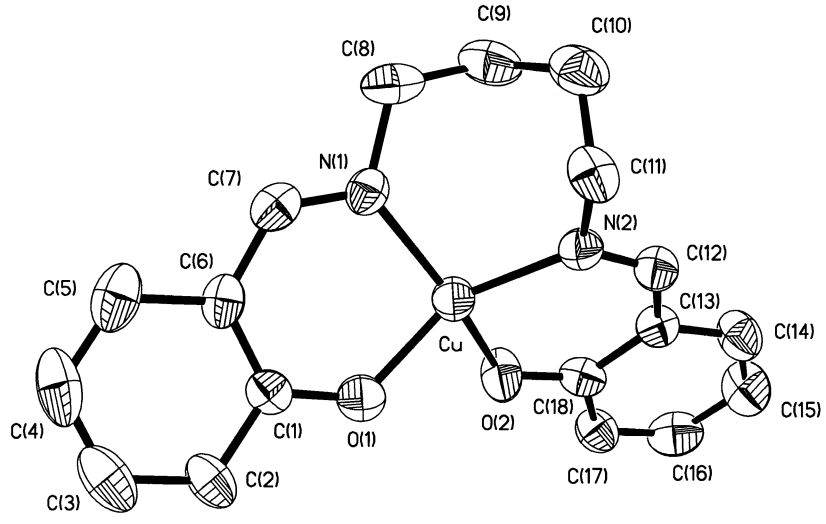

Fig. 3. Thermal ellipsoid plot at the 50% probability level for Cu(Sal-4). Hydrogen atoms are omitted for clarity.

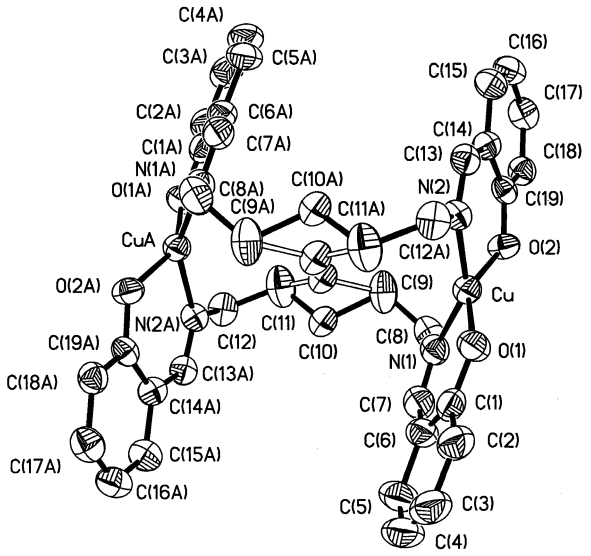

Fig. 4. Thermal ellipsoid plot for $[Cu(Sal\text{-}5)]_2$. For clarity, hydrogen atoms have been omitted and ellipsoids are shown at the 30% probability level. Disorder in the alkyl chain was modeled at 81% C(10) and 19% C(10′).

four and five CH_2 groups. Whether or not this holds for other metal centers cannot be addressed. Additionally, we have shown that different synthetic methods may produce different products, as was the case for Cu(Sal-6).

4. Supplementary material

CCDC 192631–192635 contain the supplementary crystallographic data for Cu(Sal-*n*), $n = 2$–6, respectively. These data can be obtained free of charge at http://www.ccdc.cam.ac.uk/conts/retrieving.html or from the Director, Cambridge Crystallographic Data Center (CCDC), 12 Union Road, Cambridge CB2 1EZ, UK (fax: +44-1223-336033; e-mail: deposit@ccdc.cam.ac.uk or www: http://www.ccdc.cam.ac.uk).

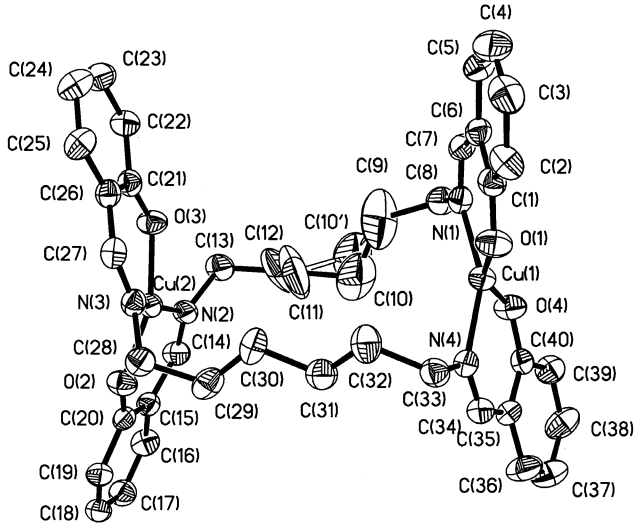

Fig. 5. Thermal ellipsoid plot for $[Cu(Sal\text{-}6)]_2$. For clarity, hydrogen atoms have been omitted and ellipsoids are shown at the 30% probability level. Disorder in the alkyl chain was modeled at 54% C(10) and 46% C(10′).

Acknowledgements

The authors wish to acknowledge the following sources of financial support: L.C.N. and J.E.K. from Santa Clara University (SCU)—IBM research grants; J.E.K. from a SCU Women in Science and Engineering-Pacific Telesis grant; K.A.H. from a SCU Chemistry Department research grant; W.E.D. and J.M.G. from NSF-REU grants CHE-9531723 and CHE-9820382, respectively.

References

[1] G.A. Kolawole, K.S. Patel, J. Chem. Soc., Dalton (1981) 1241.
[2] P.E. Riley, V.L. Pecoraro, C.J. Carrano, J.A. Bonadies, K.N. Raymond, Inorg. Chem. 25 (1986) 154.
[3] M. Mathew, A.J. Carty, G.J. Palenik, J. Am. Chem. Soc. 92 (1970) 3197.
[4] S.J. Gruber, C.M. Harris, E. Sinn, J. Inorg. Nucl. Chem. 30 (1968) 1805.
[5] S. Yamada, H. Nishikawa, H. Kuma, Sci. Rep., Coll. Gen. Educ., Osaka. Univ. 22 (1973) 45.
[6] R.H. Holm, J. Am. Chem. Soc. 82 (1960) 5632.
[7] M. Calvin, C.H. Barkelew, J. Am. Chem. Soc. 68 (1946) 2267.
[8] A.E. Martell, M. Calvin, Chemistry of the Metal Chelate Compounds, Prentice-Hall, New York, 1952, pp. 266–267.
[9] H. Weigold, B.O. West, J. Chem. Soc. (A) (1967) 1310.
[10] M. Hariharan, F.L. Urbach, Inorg. Chem. 8 (1969) 556.
[11] G.E. Batley, D.P. Graddon, Aust. J. Chem. 20 (1967) 885.
[12] D. Hall, F.H. Moore, Proc. Chem. Soc. (1960) 256.
[13] G.E. Batley, D.P. Graddon, Aust. J. Chem. 21 (1968) 267.
[14] D. Hall, T.N. Waters, J. Chem. Soc. (1960) 2644. Summary of crystallographic data: $C_{16}H_{14}N_2O_2Cu$, $M = 329.9$, monoclinic, $C2/c$, $a = 26.55(10)$ Å, $b = 6.93(2)$ Å, $c = 14.60(5)$ Å, $\beta = 97.5(5)^\circ$, $Z = 8$, $D_{calc} = 1.644$ g cm^{-3}.
[15] G.V. Panova, V.M. Potapov, I.M. Turovets, E.G. Golub, Zh. Obshch. Khim. 53 (1983) 1612; English translation: J. Gen. Chem. USSR 53 (1983) 1452.
[16] G.E. Batley, D.P. Graddon, Aust. J. Chem. 21 (1968) 1473.
[17] S.K. Shaikhutdinov, A.N. Shupik, E.M. Trukhan, J. Chem. Soc. Faraday Trans. 89 (1993) 3959.
[18] B.J. McNelis, L.C. Nathan, C.J. Clark, J. Chem. Soc., Dalton Trans. (1999) 1831.
[19] SHELXTL Software, Version 5.03, (Siemens) Bruker Analytical Systems, Madison, WI, 1994.
[20] S. Parkin, B. Moezzi, H. Hope, J. Appl. Crystallogr. 28 (1995) 53.
[21] Summary of crystallographic data for $[Cu(Sal\text{-}8)]_2$: $C_{44}H_{56}Cu_2N_4O_4$, $M = 832.01$, grn–brn parallelepiped $0.42 \times 0.18 \times 0.09$ mm, $T = 298$ K, triclinic, $P\bar{1}$, $a = 13.296(4)$ Å, $b = 14.109(4)$ Å, $c = 14.312(3)$ Å, $\alpha = 112.79(2)^\circ$, $\beta = 116.60(2)^\circ$, $\gamma = 95.59(2)^\circ$, $V = 2090.3(9)$, $Z = 2$, $D_{calc} = 1.322$ g cm^{-3}, 7915 reflections, 6944 independent reflections ($R_{int} = 0.0478$), incomplete solution (disorder not resolved; no anisotropic refinement; no H atoms) with $R_1 = 0.18$.